THE PHASE FUNCTION OF CERES AT HIGH PHASE ANGLES. Jian-Yang Li[1], A. Nathues[2], S. Mottola[3], M.C. De Sanctis[4], N. Mastrodemos[5], M.V. Sykes[2], C.T. Russell[6], C.A. Raymond[5], M. Hoffmann[2], A. Longobardo[4], M. Ciarniello[4], [1]Planetary Science Institute, Tucson, AZ, USA, jyli@psi.edu, [2]Max Planck Institute for Solar System Research, Göttingen, Germany, [3]Deutsches Zentrum für Luft- und Raumfahrt (DLR), Berlin, Germany, [4]Instituto di Astrofisica e Planetologia Spaziali, INAF, Roma, Italy, [5]Jet Propulsion Laboraotry, Pasadena, CA, USA, [6] Institute of Geophysics and Planetary Physics, University of California, Los Angeles, CA, USA.

Introduction: The phase function of a planetary surface is a fundamental light scattering property, containing clues about the physical properties of planetary surfaces regolith such as albedo, grain packing status and size, macroscopic roughness, etc. In order to fully characterize the phase function and disentangle the different effects of various properties, measurements at multiple wavelengths covering the full range of phase angles (0º – 180º) are desired. Laboratory studies suggest that the forward scattering properties contain substaintial information about the internal physical properties of regolith particles [1, 2, 3]. However, phase angles greater than 30º are not accessible from the ground for main-belt asteroids, but only with spacecraft missions.

Previous multi-spectral studies of asteroid phase functions at high phase angles (>100º) have been carried out only for Asteroids (253) Mathilde (C-type) using ground-based and the NEAR spacecraft data [4] and (433) Eros (S-type) with the NEAR data [5]. High-phase studies of some near-Earth asteroids can be performed from the ground (e.g., [6]), but with very limited wavelength range and data quality, and strongly affected by the unknown but highly irregular shape. For Ceres, the highest phase angle reachable from the ground is ~23º. Therefore, the photometric properties of almost all asteroids at high phase angles are not well understood, although a large amount of such data have been available for the Moon (e.g., [7]) and Mercury (e.g., [8, 9]).

Ceres is a C-type asteroid and the second target of NASA's Dawn mission. The Dawn spacecraft will start to orbit Ceres in April 2015. During the approach and the third rotational characterization (RC3) observations, the Framing Camera (FC, [10]) and the Visible and Infrared Spectrometer (VIR, [11]) onboard Dawn spacecraft will collect multi-spectral images of Ceres at phase angles from ~16º to ~160º (Fig. 1). These data will cover spectral range of 0.25 – 5 μm [11], ideal for carrying out a detailed study of the phase function of Ceres at high phase angles.

Expected Data: During approach, the FC and the VIR will collect images of Ceres during a series of OpNav and three rotational characterization (RC) observations (Fig. 1). The OpNavs are short (one to a few hours) observations while all RCs cover at least one full rotation of Ceres in ~9 hours. The FC will collect images through clear filter (centered at ~0.7 μm) during all OpNavs, and through all eight filters (0.44 – 0.96 μm, and clear) during RCs, while the VIR will take data during all observations, covering 0.25 – 5.0 μm, although thermal emission will probably dominate at wavelengths >3.5 – 4 μm. The full disk of Ceres will fit within the field-of-view of FC in all these planned observations, and fit within the field-of-view of VIR in early observations, allowing us to model the phase function for the average surface of Ceres.

Expected Results: We plan to perform a detailed Hapke modeling [12] for the disk-integrated phase function of Ceres at all wavelengths covered by FC and VIR. Since the data do not cover phase angles within the opposition surge, we will not be able to constrain the opposition parameters. Rather, we will focus on the modeling of the single-scattering phase function (SSPF), especially the forward scattering properties. We will adopt a two-parameter Henyey-Greenstein (H-

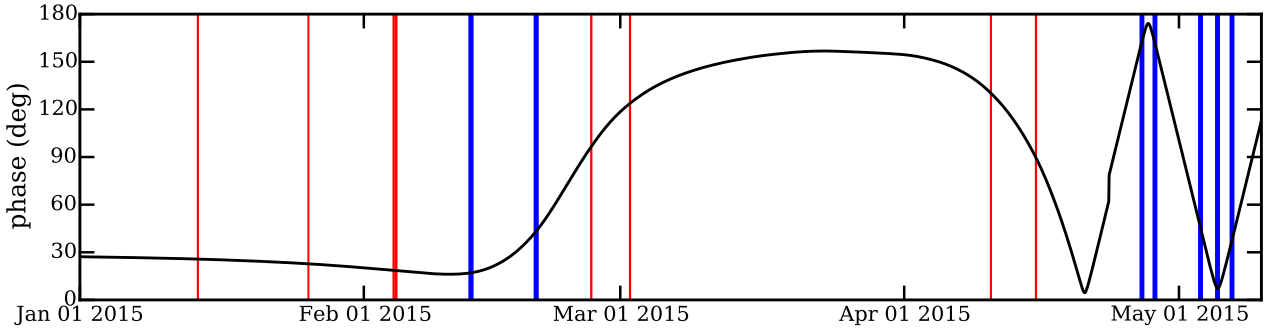

Fig. 1. The phase angle of Dawn during approach and RC3. The red vertical bars are planned OpNav observations, and the blue bars are planned RCs.

G) function to constrain the forward scattering lobe. We will use the disk-resolved images of Ceres at moderate to high phase angle to constrain the roughness, and adopt it in the modeling of SSPF.

We expect to fully constrain the SSPF of Ceres regolith particles with forward scattering by fitting the two parameters in the H-G function at wavelengths of 0.25 – 4 μm. We will then put the best-fit parameters in the "hockey-stick" plot [1, 2, 3] to compare with laboratory measurements to determine the physical properties of Ceres' regolith. With the wavelength dependency of the H-G parameters, we should be able to put constraints on the scale size of the internal structures (opaques, particle size, shape, etc) of Ceres' regolith particles. These results will provide clues about the evolution of Ceres' regolith, related to its geophysical history and micrometeorite gardening history.

One of the most significant clues on the evolution of Ceres's surface is the comparison of its roughness on different size scales. This comparison will show the effects of local impact features in contrast with global relaxation processes on one hand and small scale regolith gardening on the other. Comparison of photometric properties in the areas of potential large palimpsests may already become possible using RC3 images.

We will present the preliminary studies of the phase function of Ceres at high phase angles using Dawn approach data.

Acknowlegement: The funding for this research was provided under NASA grant NNM05AA86 through a subcontract from the University of California, Los Angeles.

References: [1] McGuire A.F. and Hapke B.W. (1995) *Icarus*, 113, 134-155. [2] Souchon A.L. et al. (2011) *Icarus*, 215, 313-331. [3] Hapke B. (2012) *Icarus*, 221, 1079-1083. [4] Clark B.E. (1999) *Icarus*, 140, 53-65. [5] Clark B.E. et al. (2002) *Icarus*, 155, 189-204. [6] Hergenrother C.W. et al. (2013) *Icarus*, 226, 663-670. [7] Kieffer H.H. and Stone T.C. (2005) *AJ*, 129, 2887-2901. [8] Domingue D.L. et al. (2010) *Icarus* 209, 101-124. [9] Domingue D.L. et al. (2011) *PSS*, 59, 1853-1872. [10] Sierks H. et al. (2011) *SSR*, 163, 263-327. [11] De Sanctis M.C. et al. (2011) *SSR*, 163, 329-367. [12] Hapke B. (2012) Theory of Reflectance and Emittance Spectroscopy (book).